

# Design, synthesis, and binding studies of bidentate Zn-chelating peptidic inhibitors of glyoxalase-I

Swati S. More and Robert Vince\*

Center for Drug Design, Academic Health Center, and Department of Medicinal Chemistry, College of Pharmacy,  
University of Minnesota, 8-123A WDH, 308 Harvard Street SE, Minneapolis, MN 55455, USA

Received 11 November 2006; revised 12 December 2006; accepted 13 December 2006  
Available online 21 December 2006

**Abstract**—The known affinity of ethyl acetoacetate (ACC) toward divalent zinc prompted us to attempt its employment as a chelating moiety in the design of glyoxalase-I inhibitors. A practical synthetic route was developed to incorporate this pharmacophore into the side chain of glutamic acid, with flexibility to allow incorporation of additional functionality at the end-stage of the synthesis. Herein, the details of this synthetic approach as well as the evaluation of the resultant  $\beta$ -keto ester compounds are reported. © 2007 Elsevier Ltd. All rights reserved.

Substantial experimental evidence exists for the inhibitory effect of endogenous  $\alpha$ -ketoaldehydes on cell growth.<sup>1</sup> Methylglyoxal, one of the simplest  $\alpha$ -ketoaldehydes, is formed by the non-enzymatic and enzymatic fragmentation of dihydroxyacetone phosphate and glyceraldehyde 3-phosphate<sup>2,3</sup> and the catabolism of threonine.<sup>4</sup> But the therapeutic use of  $\alpha$ -ketoaldehydes as potential anticancer agents is limited due to their detoxification to the corresponding aldonic acids by the glyoxalase system. This enzyme system requires reduced glutathione because the hemithioacetal formed non-enzymatically from reduced glutathione and  $\alpha$ -ketoaldehyde is the substrate for glyoxalase-I and is further converted to D-lactic acid by glyoxalase-II (Fig. 1).<sup>5</sup>

The major protective role played by the glyoxalase enzyme system prompted us to put forward a hypothesis that glyoxalase-I (Glx-I) inhibitors could be potential anticancer agents.<sup>6</sup> This was confirmed later through the development of numerous competitive and transition state analog inhibitors of Glx-I. The initial design of competitive inhibitors was based on taking advantage of the deep hydrophobic pocket in the active site of Glx-I. A large number of S-substituted alkylglutathiones<sup>7</sup> were synthesized; our S-*p*-bromobenzylglutathione (**1**)<sup>8</sup> being the most active amongst them. Further, the devel-

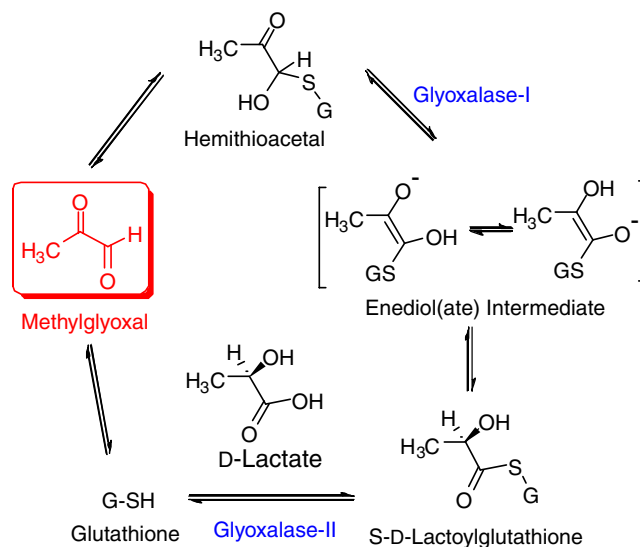
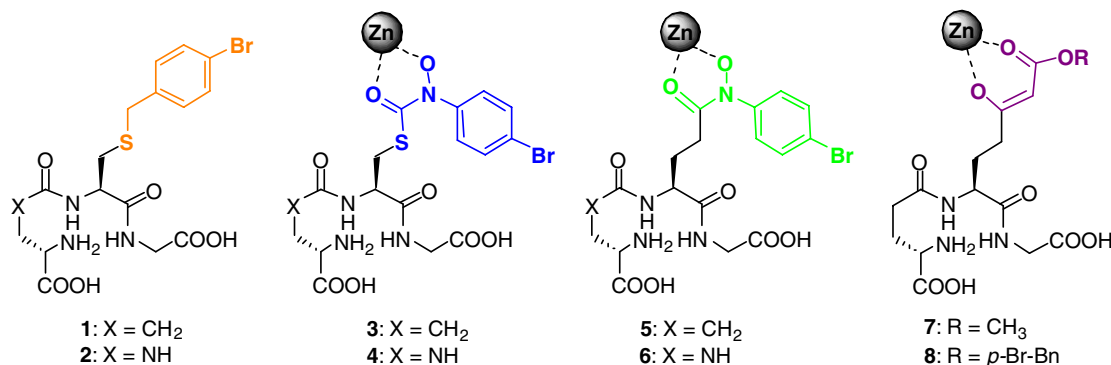


Figure 1. Glyoxalase pathway.

opment of the enediol(ate) transition state mimics, S-(*N*-aryl-*N*-hydroxycarbamoyl)glutathiones (**3**), by Creighton and Murthy<sup>9,10</sup> started a new era of more potent tight-binding Glx-I inhibitors. Enhanced potency was due to possible chelation of the hydroxamate function with the divalent zinc in the active site. But the therapeutic use of these inhibitors as anticancer agents was precluded because of their charged nature, which limited their penetration inside cells and lability

**Keywords:** Methylglyoxal; Glyoxalase; Ethyl acetoacetate; Glutathione;  $\beta$ -Keto ester; Transition-state inhibitor.

\* Corresponding author. Tel.: +1 612 6249911; fax: +1 612 6240139;  
e-mail: [vince001@umn.edu](mailto:vince001@umn.edu)



**Figure 2.** Development in the design of glyoxalase-I inhibitors.

to  $\gamma$ -glutamyltranspeptidase-mediated cleavage that led to their inactivation. The utilization of diester prodrugs of our *S-p*-bromobenzylglutathione inhibitor by Lo and Thornalley<sup>11</sup> overcame the cell-penetration problem. We recently reported upon the metabolic stability and inhibitory potency of a urea-isostere containing analog (**4**) (Fig. 2) of these tight-binding inhibitors.<sup>12</sup>

Recently, we developed a potent, tight-binding carboanalog<sup>13</sup> of hydroxamate based transition state inhibitor **3**, compound **5** ( $K_i = 6.17$  nM), and synthesized its metabolically stable analog **6** ( $K_i = 32.6$  nM) (Fig. 2) which retained the inhibitory potency. The bioactivity of this series of compounds proved that the presence of sulfur is inconsequential to the ability of these glutathione analogs to inhibit Glx-I. Abolishing the Glx-II substrate similarity of these molecules would be expected to improve their in vivo stability against the hydrolysis of the thioester function, which is mediated by Glx-II. Removal of the sulfur atom also drastically reduced the synthetic complexity, thus facilitating further structural explorations.

The hydroxamate link, however, remained a foible that could render futile the aforementioned improvements. Although a strong ligand for zinc, this hydroxamide link is quite susceptible to hydrolytic breakdown. Indeed, the poor pharmacokinetics of hydroxamate-based enzyme inhibitors have plagued drug-development efforts in many an instance. We therefore deemed worthwhile the search for an alternative zinc-chelating group that would be more stable and also be amenable to substitutions for carrying out SAR at the hydrophobic substituent. The full 4s orbital and an empty 4p orbital of zinc allow for two covalent and two dative-coordinate bonds. As a consequence, Zn(II) salts (zinc chloride and zinc acetate) are known to form stoichiometric complexes with bidentate ligands.<sup>14</sup> In glyoxalase-I, Glu99 and Glu172 fulfill the covalent bonds, while two water molecules co-ordinate to this ion.<sup>15</sup> We sought to test the possibility of displacing the two water molecules by an ethyl acetoacetate (ACC)-like bidentate ligand (Fig. 3). ACC has been known to form stable complexes with divalent zinc, some of them being robust enough to be utilized as stabilizers in vinyl halide polymers.<sup>14</sup> Our choice of ACC was also based on the potential ease in variation of the terminal alkyl substituent. The initial

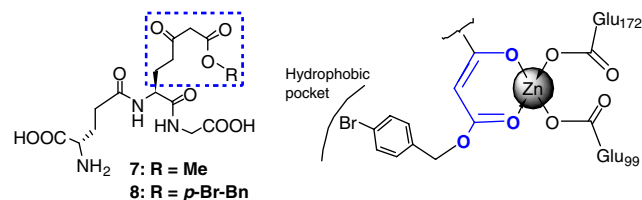


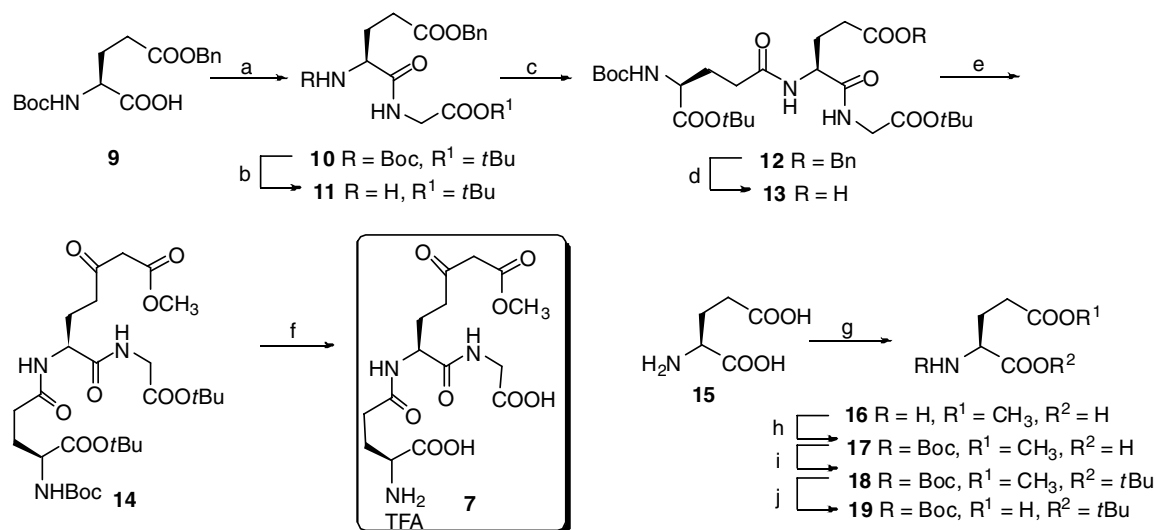
**Figure 3.** Rationale for the design of  $\beta$ -ketoester-based Glx-I inhibitors.

targets chosen were **7**, the methyl ester analog, and **8**, with the *p*-bromobenzyl substituent.

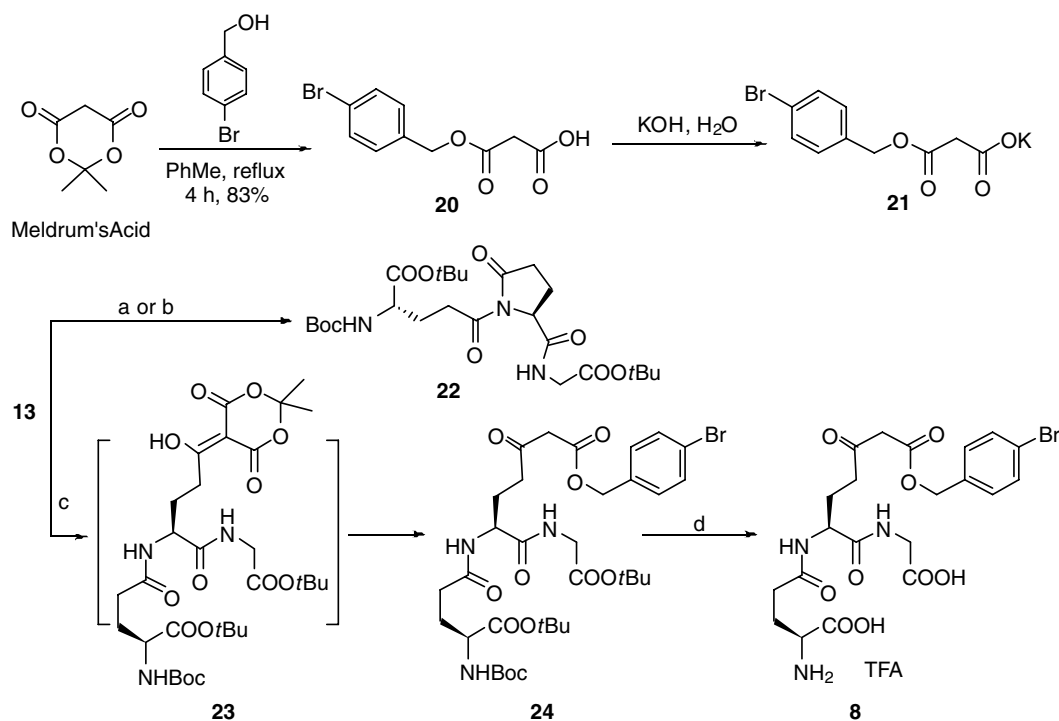
Synthesis of **7** is outlined in Scheme 1. EDC/HOBt-mediated coupling of the commercially available Boc-L-Glu(OBn)-OH with glycine *t*-butyl ester (as the HCl salt) afforded the dipeptide **10**. Selective removal of the Boc-function of dipeptide **10** in presence of the *t*-butyl ester was achieved by following the protocol of Hruby<sup>16</sup> (4 N HCl/dioxane at 0 °C). Amine **11** thus obtained was coupled to Boc-L-Glu(OH)-O*t*Bu (**19**) to obtain the tripeptide **12** in 84% yield. Compound **19** was prepared in four steps from L-glutamic acid. Regioselective side-chain methyl-esterification of glutamic acid **15** was achieved using chlorotrimethylsilane in methanol.<sup>17</sup> Amino acid **16** thus obtained was subjected to Boc protection using di-*tert*-butyl dicarbonate and *t*-butyl esterification of the carboxylic acid using *t*-BuOH/DCC-DMAP to obtain the orthogonally protected glutamic acid derivative **18**. Finally, hydrolysis of the side-chain methyl ester by lithium hydroxide gave the acid Boc-L-Glu(OH)-O*t*Bu (**19**).

Hydrogenolysis of the tripeptide **12** caused its quantitative conversion to the free acid **13**. Assembly of the  $\beta$ -keto ester<sup>18</sup> functionality was achieved by in situ conversion of acid **13** to its imidazolidine with carbonyl diimidazole (CDI), and subsequent treatment with the Mg<sup>2+</sup>-enolate of potassium monomethyl malonate to result in the formation of  $\beta$ -keto methyl ester precursor **14**. Global deprotection of protected  $\beta$ -keto ester **14** by treatment with trifluoroacetic acid lended us the title compound **7**.<sup>19</sup>

However, the same strategy was found to be inapplicable to the synthesis of  $\beta$ -ketobenzyl ester **8** (Scheme 2).



**Scheme 1.** Synthesis of **7**. Reagents and conditions: (a) HCl-GlyOtBu, EDC, HOBT, NMM, CH<sub>2</sub>Cl<sub>2</sub>, 91%; (b) 4N HCl/dioxane, 0 °C; (c) **19**, EDC, HOBT, NMM, CH<sub>2</sub>Cl<sub>2</sub>, 84%; (d) H<sub>2</sub>, 10% Pd/C, CH<sub>3</sub>OH, 86%; (e) CDI, CH<sub>3</sub>CN then MgCl<sub>2</sub>, potassium monomethyl malonate, CH<sub>3</sub>CN, 59%; (f) TFA/CH<sub>2</sub>Cl<sub>2</sub> (1:1), 79%; (g) TMSCl, rt, 97%; (h) Boc<sub>2</sub>O, Na<sub>2</sub>CO<sub>3</sub>, dioxane/H<sub>2</sub>O, 91%; (i) *t*BuOH, DCC, DMAP, CH<sub>2</sub>Cl<sub>2</sub>, 94%; (j) LiOH, THF/H<sub>2</sub>O, 84%.



**Scheme 2.** Synthesis of **8**. Reagents and conditions: (a) CDI, CH<sub>3</sub>CN then MgCl<sub>2</sub>, **21**, CH<sub>3</sub>CN, 46%; (b) CDI, THF then **21**, *i*PrMgCl, THF, 40%; (c) Meldrum's acid, DCC, DMAP, CH<sub>2</sub>Cl<sub>2</sub> then 4-bromobenzyl alcohol, benzene, reflux, 3 h, 42%; (d) TFA/CH<sub>2</sub>Cl<sub>2</sub> (1:1), 84%.

We were unable to achieve a mono-hydrolysis of di(4-bromo)-benzyl malonate to the desired potassium mono-(4-bromo)-benzyl malonate (**21**) in reasonable reaction times and yields. A faster and higher yielding (83%) method was the acylation of *p*-bromobenzyl alcohol by Meldrum's acid, followed by neutralization of the product with potassium hydroxide.<sup>20</sup> In contrast to the facile acylation observed during the synthesis of **14**, when the Mg<sup>2+</sup>-enolate of **21** was treated with the imidazole of **13**, imide **22** was isolated as the major prod-

uct. This was thought to have happened because of the slower attack of the enolate of **21** relative to the Lewis acid (Mg<sup>2+</sup>), catalyzed cyclization. In order to sidestep this facile ring-closure, we first acylated Meldrum's acid with the DCC-activated derivative of **13**, presumably forming **23** in situ, followed by addition of *p*-bromobenzyl alcohol and refluxing the reaction in benzene<sup>21</sup> for 3 hours to give **24** in a gratifying 42% yield. Global deprotection of **24** by treatment with trifluoroacetic acid gave the second target compound **8**.<sup>22</sup>

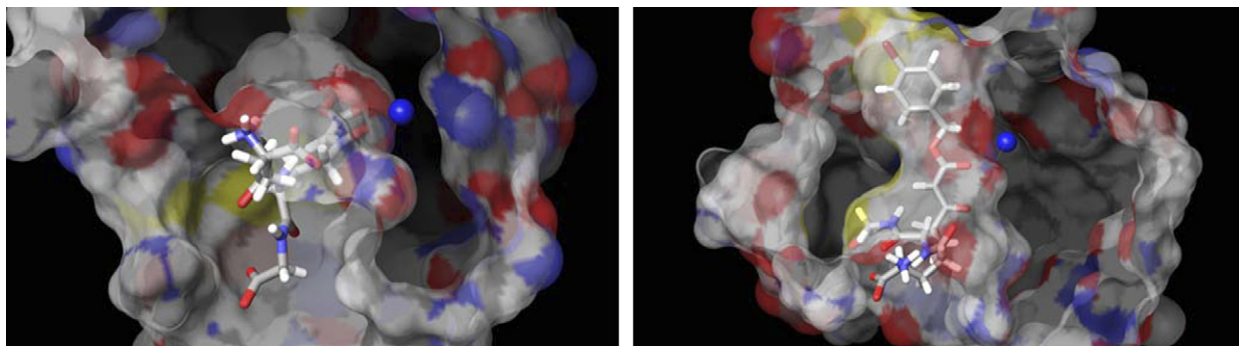


**Figure 4.** Predicted binding conformations of  $\beta$ -keto esters **7** (left) and **8** (right) in the glyoxalase I active site.

The  $\beta$ -ketoesters **7** and **8** were examined for their ability to inhibit yeast glyoxalase-I. Initial rates of the enzymatic reaction were measured by following the increase in absorption at 240 nm in 0.05 M phosphate buffer (pH 6.6). Methylglyoxal, GSH, inhibitor, and buffer were then added to the cell and allowed to equilibrate at 30 °C for 6 min (to allow formation of the hemimercaptal) before addition of the enzyme. The concentrations of the hemimercaptal were calculated using the dissociation constant,  $3.1 \times 10^{-3}$  M, as previously determined for this equilibrium reaction.<sup>8</sup> Analysis of the enzyme kinetics showed that  $\beta$ -ketoesters were competitive inhibitors of Glx-I, with  $K_i$  values of  $112.44 \pm 36.23$   $\mu$ M for **7** and  $66.88 \pm 22.84$   $\mu$ M for **8**. The  $K_m$  for the hemimercaptal, the Glx-I substrate, was 0.5 mM, which is in close agreement with the literature value.<sup>23</sup>

The very fact that compounds **7** and **8** were inhibitors of Glx-I signifies that the novel  $\beta$ -ketoester function does hold potential in the design of inhibitors for this enzyme. We then began investigating lowered potency of these inhibitors when compared to the hydroxamates. One way would be to predict in silico the binding conformation. X-ray crystallographic data on human glyoxalase-I complexed with S-(*N*-hydroxy-*N*-*p*-iodophenylcarbamoyl)glutathione have been reported by Cameron et al.<sup>15</sup> This was used as the starting point for the docking of our inhibitors. Glide, as implemented in the Maestro software, was used for this docking. Validation of this docking was obtained by docking the original ligand, S-(*N*-hydroxy-*N*-*p*-iodophenylcarbamoyl)glutathione, in Glx-I active site. RMSD of 0.8810 Å between docked and crystallographically determined conformation of this ligand validated the reliability of our docking protocol. When compound **7** was docked in the Glx-I active site (Fig. 4), the tripeptide backbone overlaid perfectly with the original ligand in the X-ray crystal structure. The glutamine terminal showed the carboxylate forming a salt bridge interaction with Arg37, Arg122 and hydrogen bonding with carboxamide protons of Asn103. The amino terminus is also involved in hydrogen bonding with carboxamide oxygen of Asn103. The carboxylate oxygens of the glycine residue are within hydrogen-bonding distance of the main-chain nitrogens of Met157 and Lys156. The O<sub>e1</sub> atom of Glu99 and the N<sub>e2</sub> atom of His126 as well as the  $\beta$ -keto ester functionality form the coordination sphere of

the zinc metal. However, a hydrophobic substituent to fill the large hydrophobic pocket in the glyoxalase active site was lacking, which could explain the relatively high  $K_i$ .

Docking of compound **8** showed similar interactions of the  $\beta$ -keto ester functionality with the zinc ion (Fig. 4). Though it had the advantage of having a *p*-bromobenzyl substituent to fill the large hydrophobic pocket, the positioning of this substituent was found to be in collision with the surface of the enzyme. A slight increase in the number of atoms as compared to compounds **5** and **6** is probably responsible for the displacement of the tripeptide backbone from its ideal position. Thus, the inability of **8** to drastically improve upon **7** may stem in part from the inaccurate spatial orientation of its hydrophobic substituent. In addition, a reviewer cited the lower ability of the  $\beta$ -ketoester function to coordinate zinc as a reason for decreased activity.

In summary, we have identified the  $\beta$ -ketoester function as a possible zinc-chelating component of Glx-I inhibitors. We have also overcome the key problems in the construction of  $\beta$ -ketoester analogs of glutathione. Our final synthetic approach should be amenable to the introduction of a large number of substituents at the hydrophobic portion. The results of docking indicate that the  $\beta$ -ketoester function does coordinate to zinc, but the placement of the hydrophobic substituent might be inaccurate. Subsequent design and synthesis efforts are currently in progress to improve upon the potency of these inhibitors through correct placement of the hydrophobic substituent.

#### Acknowledgment

This work was supported by the funding from the Center for Drug Design, Academic Health Center, University of Minnesota.

#### References and notes

1. Fraval, H. N.; McBrien, D. C. *J. Gen. Microbiol.* **1980**, *117*, 127.
2. Phillips, S. A.; Thornalley, P. J. *Eur. J. Biochem.* **1993**, *212*, 101.

3. Casazza, J. P.; Felver, M. E.; Veech, R. L. *J. Biol. Chem.* **1984**, 259, 231.
4. Lyles, G. A.; Chalmers, J. *Biochem. Pharmacol.* **1992**, 43, 1409.
5. (a) Thornalley, P. J. *Biochem. J.* **1990**, 269, 1; (b) Hertz, L.; Gerald, A. D. *J. Neurosci. Res.* **2004**, 79, 11.
6. Vince, R.; Wadd, W. B. *Biochem. Biophys. Res. Commun.* **1969**, 35, 593.
7. Vince, R.; Daluge, S. *J. Med. Chem.* **1971**, 14, 35.
8. Vince, R.; Daluge, S.; Wadd, W. B. *J. Med. Chem.* **1971**, 14, 402.
9. Murthy, N. S. R. K.; Bakeris, T.; Kavarana, M. J.; Hamilton, D. S.; Lan, Y.; Creighton, D. J. *J. Med. Chem.* **1994**, 37, 2161.
10. Hamilton, D. S.; Creighton, D. J. *J. Biol. Chem.* **1992**, 267, 24933.
11. Lo, T. W. C.; Thornalley, P. *Biochem. Pharmacol.* **1992**, 44, 2357.
12. More, S. S.; Vince, R. *Bioorg. Med. Chem. Lett.* **2006**, 16, 6039.
13. More, S. S.; Vince, R. In preparation.
14. (a) Grummitt, O.; Perz, J.; Mehaffey, J. *Org. Prep. Proced. Int.* **1972**, 4, 299; (b) Backus, A. C.; Wood, L. L. *Fr. 1546264*. **1968**.
15. Cameron, A. D.; Ridderstrom, M.; Olin, B.; Kavarana, M. J.; Creighton, D. J.; Mannervik, B. *Biochemistry* **1999**, 38, 13480.
16. Han, G.; Tamaki, M.; Hruby, V. J. *J. Pept. Res.* **2001**, 58, 338.
17. Ager, D. J.; Babler, S.; Erickson, R. A.; Froen, D. E.; Kittleson, J.; Pantaleone, D. P.; Prakash, I.; Zhi, B. *Org. Process Res. Dev.* **2004**, 8, 72.
18. Bonnaud, B.; Funes, P.; Jubault, N.; Vacher, B. *Eur. J. Org. Chem.* **2005**, 15, 3360.
19. Spectral data of compound 7:  $^1\text{H}$  NMR (300 MHz,  $\text{CDCl}_3/\text{CF}_3\text{COOD}$ )  $\delta$  4.20–4.18 (m, 1H,  $\alpha\text{-CH:Glu}$ ), 3.92 (m, 1H,  $\alpha\text{-CH:Glu}$ ), 3.89 (d,  $J = 6.6$  Hz, 2H,  $\text{CH}_2\text{:Gly}$ ), 3.59 (s, 3H,  $\text{OCH}_3$ ), 3.34 (s, 2H,  $\text{C(=O)CH}_2\text{C(=O)}$ ), 2.78–2.54 (m, 2H,  $\gamma\text{-CH}_2\text{C(=O)CH}_2$ ), 2.25–2.02 (m, 3H,  $\gamma\text{-CH}_2\text{:Glu}$ ,  $\beta\text{-CH}_2\text{:Glu}$ ), 1.97–1.73 (m, 3H,  $\gamma\text{-CH}_2\text{:Glu}$ ,  $\beta\text{-CH}_2\text{:Glu}$ );  $^{13}\text{C}$  NMR (75 MHz,  $\text{CDCl}_3/\text{CF}_3\text{COOD}$ )  $\delta$  202.3 ( $\text{CH}_2\text{C(=O)CH}_2$ ), 174.2, 174.0, 172.5, 172.2, 170.3 ( $\text{C(=O)}$ ), 54.0, 53.5 ( $\alpha\text{-C:Glu}$ ), 50.2 ( $\text{C(=O)CH}_2\text{C(=O)}$ ), 42.2 ( $\text{CH}_2\text{:Gly}$ ), 39.6 ( $\text{CH}_2\text{C(=O)CH}_2$ ), 31.8 ( $\gamma\text{-C:Glu}$ ), 29.3, 27.2 ( $\beta\text{-C:Glu}$ ); ESI HRMS 390.1531 ( $\text{M}+\text{H}$ ) $^+$ ,  $\text{C}_{15}\text{H}_{23}\text{N}_3\text{O}_9+\text{H}^+$  requires 390.1512; Reverse phase HPLC was run on Varian Microsorb column (C18, 5  $\mu$ , 4.6  $\times$  250 mm) using two solvent systems with 0.5 mL/min flow rate and detected at 254 nm. Solvent system 1: 0.04 M TEAB (triethylammonium bicarbonate) in water/70% acetonitrile in water = 1/1,  $t_R = 4.83$  min, purity = 99.6%. Solvent system 2: 0.04 M TEAB in water/70% acetonitrile in water = 20–100% B linear,  $t_R = 5.41$  min, purity = 96.27%.
20. Felder, D.; Nava, M. G.; Del, P. C. M.; Eckert, J.; Luccisano, M.; Schall, C.; Masson, P.; Gallani, J.; Heinrich, B.; Guillon, D.; Nierengarten, J. *Helv. Chim. Acta* **2002**, 85, 288.
21. Sun, G.; Fecko, C. J.; Nicewonger, R. B.; Webb, W. W.; Begley, T. P. *Org. Lett.* **2006**, 8, 681.
22. Spectral data of compound 8:  $^1\text{H}$  NMR (300 MHz,  $\text{CD}_3\text{OD}/\text{CF}_3\text{COOD}$ )  $\delta$  7.59 (d,  $J = 9.0$ , 2H, Ar), 7.49 (d,  $J = 8.7$  Hz, 2H, Ar), 5.10 (s, 2H,  $\text{CH}_2\text{Ph}$ ), 4.18–4.10 (m, 1H,  $\alpha\text{-CH:Glu}$ ), 3.98 (m, 1H,  $\alpha\text{-CH:Glu}$ ), 3.89 (m, 2H,  $\text{CH}_2\text{:Gly}$ ), 3.61 (s, 2H,  $\text{C(=O)CH}_2\text{C(=O)}$ ), 2.74–2.69 (m, 2H,  $\gamma\text{-CH}_2\text{C(=O)CH}_2$ ), 2.36–1.79 (m, 6H,  $\gamma\text{-CH}_2\text{:Glu}$ ,  $\beta\text{-CH}_2\text{:Glu}$ );  $^{13}\text{C}$  NMR (75 MHz,  $\text{CD}_3\text{OD}/\text{CF}_3\text{COOD}$ )  $\delta$  202.6 ( $\text{CH}_2\text{C(=O)CH}_2$ ), 175.3, 174.5, 174.1, 172.2, 171.6 ( $\text{C(=O)}$ ), 136.1, 132.2, 130.1, 123.4 ( $\text{C}_{\text{Ar}}$ ), 66.6 ( $\text{CH}_2\text{Ph}$ ), 54.1, 53.7 ( $\alpha\text{-C:Glu}$ ), 50.6 ( $\text{C(=O)CH}_2\text{C(=O)}$ ), 42.1 ( $\text{CH}_2\text{:Gly}$ ), 39.4 ( $\text{CH}_2\text{C(=O)CH}_2$ ), 31.8 ( $\gamma\text{-C:Glu}$ ), 28.6, 27.3 ( $\beta\text{-C:Glu}$ ); ESI HRMS 544.0955 ( $\text{M}+\text{H}$ ) $^+$ ,  $\text{C}_{21}\text{H}_{27}\text{BrN}_3\text{O}_9+\text{H}^+$  requires 544.0931; Reverse phase HPLC was run on Varian Microsorb column (C18, 5  $\mu$ , 4.6  $\times$  250 mm) using two solvent systems with 0.5 mL/min flow rate and detected at 254 nm. Solvent system 1: 0.04 M TEAB (triethylammonium bicarbonate) in water/70% acetonitrile in water = 1/1,  $t_R = 5.68$  min, purity = 99.9%. Solvent system 2: 0.04 M TEAB in water/70% acetonitrile in water = 20–100% B linear,  $t_R = 14.46$  min, purity = 98.9%.
23. Vince, R.; Brownell, J.; Akella, L. B. *Bioorg. Med. Chem. Lett.* **1999**, 9, 853.